Proceedings of the ASME 2017 Power and Energy Conference
PowerEnergy2017
June 25-30, 2017, Charlotte, North Carolina, USA

PowerEnergy2017-3377

HEAT TRANSFER MODELS OF MOVING PACKED-BED PARTICLE-TO-sCO_2 HEAT EXCHANGERS

Kevin J. Albrecht
Sandia National Laboratories
Albuquerque, NM, USA

Clifford K. Ho
Sandia National Laboratories
Albuquerque, NM, USA

ABSTRACT

Particle-based concentrating solar power (CSP) plants have been proposed to increase operating temperature for integration with higher efficiency power cycles using supercritical carbon dioxide (sCO_2). The majority of research to date has focused on the development of high-efficiency and high-temperature particle solar thermal receivers. However, system realization will require the design of a particle/sCO_2 heat exchanger as well for delivering thermal energy to the power-cycle working fluid. Recent work has identified moving packed-bed heat exchangers as low-cost alternatives to fluidized-bed heat exchangers, which require additional pumps to fluidize the particles and recuperators to capture the lost heat. However, the reduced heat transfer between the particles and the walls of moving packed-bed heat exchangers, compared to fluidized beds, causes concern with adequately sizing components to meet the thermal duty. Models of moving packed-bed heat exchangers are not currently capable of exploring the design trade-offs in particle size, operating temperature, and residence time. The present work provides a predictive numerical model based on literature correlations capable of designing moving packed-bed heat exchangers as well as investigating the effects of particle size, operating temperature, and particle velocity (residence time). Furthermore, the development of a reliable design tool for moving packed-bed heat exchangers must be validated by predicting experimental results in the operating regime of interest. An experimental system is designed to provide the data necessary for model validation and/or to identify where deficiencies or new constitutive relations are needed.

INTRODUCTION

Using particles as a heat transfer fluid has been identified as a potential path toward increasing operating temperature of CSP plants [1, 2] to enable the use of high efficiency power cycles such as sCO_2 [3]. However, many questions remain about the design of such systems and performance of the components including the particle solar thermal receiver as well as the particle/sCO_2 heat exchanger. Much of the work to date has focused on the development of high-temperature and high-efficiency particle solar thermal receivers [4, 5, 6, 7], however, particle/sCO_2 heat exchanger development is required for system realization. Model based performance evaluation of such devices is necessary for adequately sizing components leading to accurate cost predictions. Without reliable heat exchanger performance models, the design and cost analysis of the system is subject to large uncertainty.

Recent work has identified fluidized bed heat exchangers to be potentially cost prohibitive due to the necessary turbomachinery for providing fluidization gas as well as the recuperative heat exchangers to prevent large thermal loss from the fluidization gas. Moving packed-bed particle heat exchangers provide a potential alternative [8], which avoid both of the high cost components in fluidized beds. However, moving packed-bed heat exchangers are commonly known to have significantly reduced heat transfer coefficients in comparison to fluidized bed heat exchangers. Therefore, the required heat transfer surface area will be larger for a moving packed-bed heat exchanger for a given thermal duty.

The reduced heat transfer coefficients present in moving packed-bed heat exchangers can be explained by the surface renewal theory that has been discussed by Mickley and Fairbanks [9] and Chen et al. [10]. Fluidized beds enhance heat transfer by continually refreshing particles that have been cooled by the heat transfer surface with high temperature particles in the bulk flow. This allows for larger temperature gradient driving forces to be maintained at the heat exchanger surface. The quantitative improvement in heat transfer is proportional to the frequency of this surface renewal process. In a moving packed-bed heat exchanger, the particles contacting the heat exchanger surface are not continuously refreshed and the heat transfer is limited by the thermal conductivity of the bulk particulate material. In addition, moving bed experimental results have shown that as the contacting time between the solid and heat exchanger surface increases, the convection coefficient drops due to progressively decreasing temperature gradients at the heat exchange surface. Therefore, current literature values for moving

packed-bed heat transfer coefficients cause concern with the design of large scale (high residence time) heat exchangers.

PRIOR EXPERIMENTAL WORK

The heat transfer coefficients of moving packed-bed heat exchangers have been experimentally measured and found to have a strong dependence on residence time, bulk thermal conductivity, and particle diameter. The following section reviews the relevant studies and their findings on important parameters in design of moving packed-bed heat exchangers.

Sullivan and Sabersky [11] measured moving-bed heat transfer coefficients from vertical plates and interpreted the experimental result by considering both a discrete particle model and single-component continuum model for a semi-infinite domain. The findings suggest that there are two important thermal resistances to characterize heat transfer, which include the bulk thermal conductivity and the particle-wall contact resistance. Depending on the flow regime, the importance of the two resistances can change.

Denloye and Botterill [12] measured heat transfer coefficients in a vertical column and varied particle size, interstitial gas, gas pressure, and particle flow velocity. Their findings indicated particle size was most important parameter in which smaller particles increased the heat transfer coefficient through decreasing the wall contact resistance. Gas phase thermal conductivity was also observed to have a large impact and improvements with pressurizing the bed were also observed. Enhanced heat transfer was also observed when using particles with a much larger size distribution due to decreased voidage in the bulk and near-wall regions.

Spelt et al. [13] extended the work of Sullivan and Sabersky [11] to external flow on an inclined plane and found heat transfer coefficients begin to diminish if particle velocity is increased and a peak in the Nusselt number is observed. The diminished heat transfer was attributed to increased voidage in the near-wall region with high particle velocities.

Obuskovic [14] measured moving-bed heat transfer coefficients from a vertically oriented tube. The heat transfer coefficients were found to improve with decreasing residence time (increasing velocity). Visualization experiments also indicated that transverse particle motion to the bulk flow direction was not important to consider and the moving packed-bed of particles approximates plug flow.

Golob [15] measured heat transfer coefficients for external flows of particles over heated surfaces both with and without fins. The measured heat transfer coefficients significantly increased as particle diameter decreased. In addition, heat transfer coefficients were observed to decrease for the finned surfaces.

Most recently Baumann and Zunft [8] measured heat transfer coefficients of a moving packed-bed heat exchanger with staggered horizontally oriented tubes. Their measurements indicated that tube spacing and particle mass flow rate are important considerations. Closely spaced tubes and high mass flow rates led to increased velocities and decreased residence times that were shown to enhance heat transfer coefficients.

Many of the experimental studies on heat transfer coefficients have identified bulk particle thermal conductivity, interstitial gas phase thermal conductivity, particle diameter, and residence time as important consideration in the design of moving packed-bed heat exchangers. The interdependence of the particle diameter and gas phase thermal conductivity and their combined effect on bulk particle thermal conductivity has been discussed by Yagi and Kunii [16] and Vargas and McCarthy [17]. Baumann and Zunft [18] have also made experimental measurements of bulk thermal conductivity and have shown larger particle diameters improve bulk thermal conductivity and radiation can have a significant effect at elevated temperature (>400^{o}C). However, the majority of experimental studied have identified improved packed-bed heat transfer coefficients with decreasing particle diameter due to reduced particle-wall contact resistance. Therefore, a trade-off must exist in the optimal particle diameter, which will provide the best heat transfer performance, depending on the geometry and operating conditions of the heat exchanger.

PRIOR HEAT EXCHANGER MODELING WORK

Models of the heat transfer process of moving packed-bed heat exchangers have been reported in the literature. However, the majority of these models have been developed with properties that are specific to a single application and do not yield a robust design tool capable of rapid simulation.

Botterill and Denloye [19] developed a model for the heat transfer in a stationary packed-bed. The heat transfer process was captured through implementing two separate regions in the model of a single component continuum to divide the near-wall region from the bulk, which will differ in effective thermal conductivity. The near-wall region typically has a higher voidage than the bulk that leads to lower effective thermal conductivities.

Park [20] presented general heat exchanger effectiveness plots for different flow configurations, which were calculated from a single-component continuum model. The performance was quantified in terms of non-dimensional quantities, Biot number and inverse Graetz number.

Henda and Falcioni [21] developed a moving packed-bed heat exchanger model for Nickel processing. One- and two-component continuum models were compared and no significant difference between the approaches was found. Additionally, the heat transfer is represented by a specified wall temperature profile rather than modeling a secondary fluid temperature distribution.

Most recently Baumann and Zunft [22] reported on the use of CFD tools to represent the hydrodynamics of a moving packed-bed heat exchanger. The model was compared to particle image velocimetry (PIV) measurements of horizontal tubes. The Eulerian-Eulerian model captured the velocity profile around the tubes except for in the void region directly below the tube. However, it was concluded that the Eulerian-Eulerian model is well suited for simulating moving packed beds and future work should be directed at thermal analysis.

Packed-bed heat exchanger modeling work to date has typically relied on the use of a single-component continuum

models with effective properties. Robust numerical models of moving packed-bed heat exchanger performance are not currently available in the literature. Models, which are capable of rapid design iterations, to explore the effects of particle diameter and heat exchanger geometry would provide a novel contribution to the literature. This paper details the development of a moving packed-bed heat exchanger model capable of evaluating the effect of particle size, operating temperature, and particle velocity on performance directed at the specific application of particle/sCO_2 heat exchanger for CSP.

ANALYTICAL SOLUTION APPROACH

From the existing literature on experimental evaluation of moving packed-bed heat transfer coefficients, velocity or particle residence (contacting) time has been identified as an important design variable. This causes concern in the development of large scale heat exchangers in which high residence times are necessary to cool particles from the desired inlet to outlet temperature. Therefore, the following section details the analytical solution approach and explains the shortcomings of using a semi-infinite model to represent an internal flow (bounded domain).

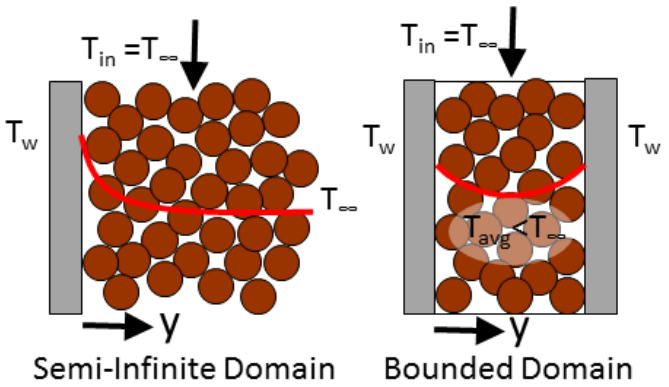

Figure 1: Illustration of moving packed-bed heat transfer in a semi-infinite and bounded domain with constant temperature wall boundary condition

Interpretation of heat transfer behavior of moving packed-beds has historically relied on analytical solutions of 1-D transient heat transfer problems. This approach assumes the particles behave as a one-component continuum and the temperature distribution can be determined through solving the heat diffusion equation (Eqn. (1)) with effective transport properties. The heat diffusion equation has many known solutions and the transient term can be converted into a convective flow through the substitution, $u\frac{\partial T}{\partial x}=\frac{\partial T}{\partial t}$, which leads to a two-dimensional temperature distribution of the domain.

$$\frac{\partial T}{\partial t}=\alpha\frac{\partial^2 T}{\partial y^2} \tag{1}$$

For a semi-infinite domain $\left(T(x,\infty)=T_\infty\right)$, Sullivan and Sabersky [11] have shown this analysis produces an average Nusselt number $\left(\overline{Nu}_L=\bar{h}L/k\right)$ given by

$$\overline{Nu}_L=\frac{2}{\sqrt{\pi}}\sqrt{Pe_L} \tag{2}$$

where the Peclet number is defined as $Pe_L=uL/\alpha$. The details of the similarity solution can be found in Bird et al. [23].

Much of the prior work on packed-bed heat transfer has identified that flows with long residence times $\left(\tau=L/u\right)$ result in diminished heat transfer coefficients. Through substitution into Eqn. (2), the average heat transfer coefficient can be shown to be inversely proportional to the square root of residence time.

$$\bar{h}=2\sqrt{\frac{u\rho c_p k}{\pi L}}=2\sqrt{\frac{\rho c_p k}{\pi\tau}} \tag{3}$$

From this analysis, one would conclude that large-scale moving packed-bed heat exchangers, which have large residence times, should have low convection coefficients and therefore poor heat transfer performance. In addition, the trends of the correlation have been confirmed experimentally through direct measurements of wall temperature and heat flux to infer the heat transfer coefficient in granular flows. This result is true for geometries that are well represented as a semi-infinite domain. However, for internal flow, which has a bounded domain, the Nusselt number will approach a constant as it does with fully developed viscous flow [24]. This has been overlooked in the field of granular flow due to the difficulty in making local temperature measurements and using the solid inlet temperature $\left(T_{s,in}\right)$ as the local temperature to calculate the convection coefficient. Typically, a good approximation for small scale experimental data is a semi-infinite domain. In other words, the assumption that the mean temperature of the particles $\left(T_{s,avg}\right)$ is not significantly changed by the heat addition $\left(T_{s,in}\approx T_{s,avg}\right)$. Under such conditions, using the heat transfer coefficient definition given by Eqn. (4) is applicable for data processing. However, if the average temperature of the solid significantly departs from the inlet temperature, as in internal flow (bounded domain), the local temperature driving force is not well represented by Eqn. (4). The local heat transfer coefficient for internal flow must be calculated based on the local average solid and wall temperature difference (Eqn. (5)) [25].

$$h_{sw}(x)=q''(x)/\left(T_{s,in}-T_w(x)\right) \tag{4}$$

$$h_{sw}(x)=q''(x)/\left(T_{s,avg}(x)-T_w(x)\right) \tag{5}$$

A solution for the heat diffusion equation in a bounded domain is necessary to capture the effects of the changing average temperature of the particles and calculate the local heat transfer coefficient by Eqn. (5). An analytical solution for the heat diffusion equation within a bounded domain does exist,

however, it results in an infinite series, which must be evaluated numerically to obtain the temperature distribution and extract the heat transfer coefficient and Nusselt numbers. The details of this solution can be found in Carslaw and Jager [26] for both constant temperature and constant heat flux boundary conditions. The Nusselt number $\left(\overline{Nu}_{Dh} = \bar{h}D_h/k\right)$ calculated from the analytical solution is plotted with respect to the inverse Graetz number $\left(Gz^{-1} = \frac{L}{Pe_{Dh}D_h}\right)$ in Figure 2 and Figure 3 for the constant wall heat flux and temperature boundary conditions, respectively. From the figures, the plug flow Nusselt number can be observed to asymptotically approach values of 9.87 and 12.0 for the constant temperature and heat flux boundary conditions, respectively. This result contradicts the typical conclusion that increased residence time decreases the heat transfer coefficient. Although the Nusselt number is observed to rapidly decrease in the entrance region, a constant value is approached after the flow is thermally developed. This is a direct result of solving for the temperature distribution in a bounded domain and determining the heat transfer coefficient using the definition of Eqn. (5) in which the driving force is the temperature difference between the wall and average solid temperature.

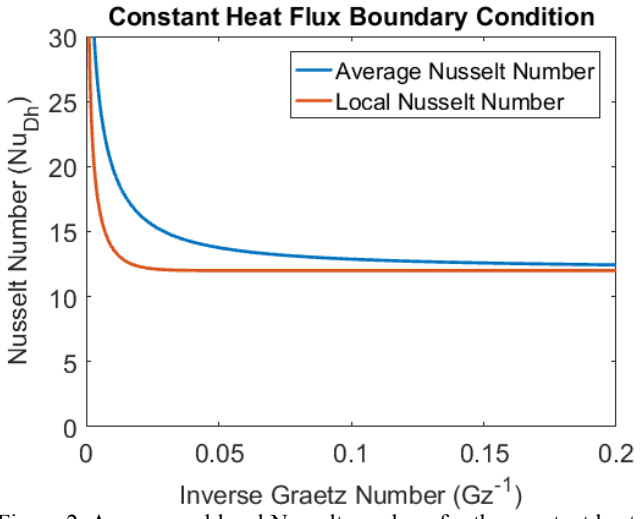

Figure 2: Average and local Nusselt numbers for the constant heat flux boundary condition as a function of inverse Graetz number

The difference between the two methods of quantifying the heat transfer coefficient (bounded domain and semi-infinite) become important when considering the performance of a heat exchanger. Heat exchanger performance can be quantified based on the overall heat transfer coefficient (U), which can be approximated by an equivalent resistance network

$$U = \left(\frac{1}{h_{sw}} + \frac{t_{HX}}{k_{HX}} + \frac{1}{h_{CO_2}}\right)^{-1} \tag{6}$$

where t_{HX} is the heat exchanger thickness, k_{HX} is the heat exchanger thermal conductivity, and h_{CO_2} is the sCO_2 convection coefficient. Typically, the overall heat transfer coefficient is extracted from the heat exchanger conductance (UA) by dividing by the heat transfer area. The conductance can be obtained from the heat transfer (Q) and the log mean temperature difference (ΔT_{lm}) (LMTD) for the particular flow configuration (Eqns. (7) and (8)). The LMTD can be thought of as the average local temperature difference over the length of the heat exchanger. Therefore, if the particle heat transfer coefficient is not accurately quantified based on the local temperature difference (Eqn. (5)), the overall heat transfer coefficient of the heat exchanger will appear to disagree with the particle heat transfer coefficient that has typically been reported in literature data.

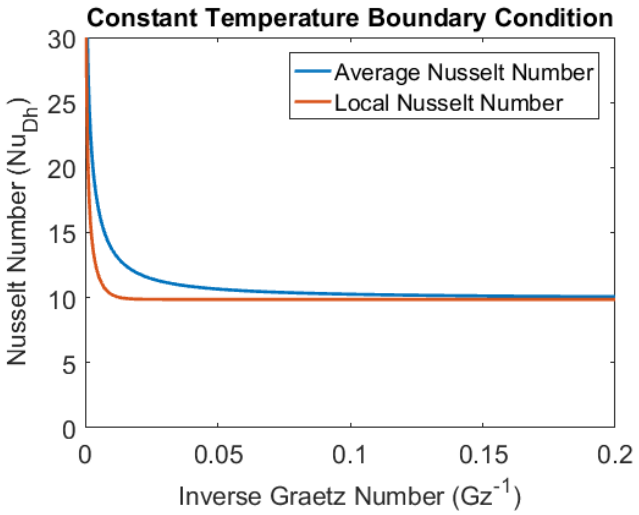

Figure 3: Average and local Nusselt numbers for the constant wall temperature boundary condition as a function of inverse Graetz number

$$\Delta T_{lm} = \frac{\left(T_{s,out} - T_{CO_2,in}\right) - \left(T_{s,in} - T_{CO_2,out}\right)}{\ln\left(\frac{T_{s,out} - T_{CO_2,in}}{T_{s,in} - T_{CO_2,out}}\right)} \tag{7}$$

$$Q = UA \cdot \Delta T_{lm} \tag{8}$$

PARTICLE/sCO_2 HEAT EXCHANGER MODEL DEVELOPMENT

The analytical solutions presented in the previous section provide insight into the expected particle-wall heat transfer coefficients. However, the model must include an energy balance for the sCO_2 to accurately simulate the heat exchanger, which provides the boundary conditions for the 2-D single-component continuum moving packed-bed model. In addition, the thermophysical properties of the sCO_2 and moving packed are not constant and the variation must be captured over the heat exchanger. Therefore, the partial differential equations become highly non-linear and a numerical solution is necessary.

The model solves the conjugate heat transfer problem between the moving packed-bed of particles and counter-flow sCO_2 fluid in a shell-and-plate configuration (Figure 4). A 1-D steady-state conservation of energy equation for the sCO_2 is

given by Eqn. (9) and a 2-D steady-state conservation of energy equation for the particles (subscript s) is given by Eqn. (10).

$$\rho_{CO_2} v_{CO_2} c_{p,CO_2} \frac{dT_{CO_2}}{dx} = \frac{2q''}{hc_{CO_2}} \tag{9}$$

$$\rho_s v_s c_{p,s} \frac{\partial T_s}{\partial x} = \frac{\partial}{\partial y}\left(k_{s,eff} \frac{\partial T_s}{\partial y} \right) \tag{10}$$

The boundary conditions for the differential equations can be expressed as

$$T_{CO_2}(H) = T_{CO_2,in} \tag{11}$$

$$T_s(0,y) = T_{s,in} \tag{12}$$

which specify the inlet temperatures of the sCO_2 and particle flows. In addition to the inlet boundary conditions, outlet boundary conditions are also specified for the sCO_2 and particle flow as

$$T_{CO_2}(0) = T_{CO_2,out} \tag{13}$$

$$\frac{1}{hc_s}\int_0^{hc_s} T_s(H,y)dy = T_{s,out} \tag{14}$$

where the velocities (v_{CO_2}, v_s) become variables that must be solved for to satisfy the conditions.

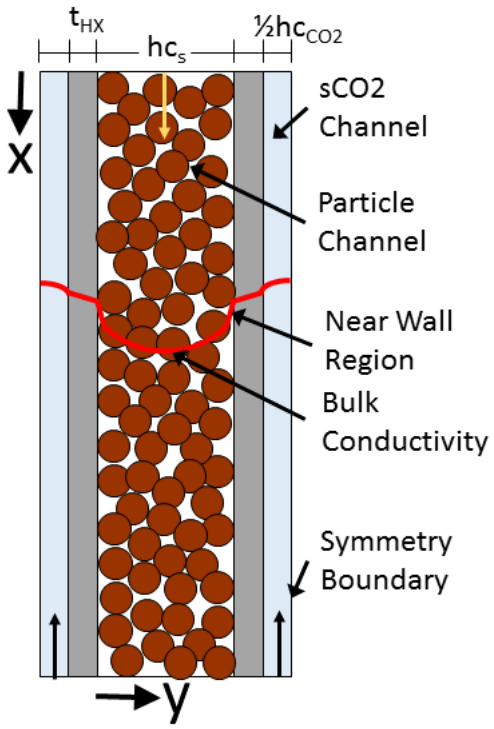

Figure 4: Illustration of the shell-and-plate moving packed-bed particle-to-sCO_2 heat exchanger model

The 2-D particle conservation of energy equation assumes the particles behave as a single-component continuum in which the bulk thermal conductivity $(k_{s,eff})$ is an appropriate way to characterize the particulate media. The limiting factor of heat transfer in moving packed-bed heat exchangers has typically been attributed to the low thermal conductivity of the bulk particulate material. Therefore, it becomes important to include the transverse (y-direction) temperature distribution in the particles to capture the thermal resistance of transferring heat from the particles to the sCO_2. The effective thermal conductivity of the bulk particulate material can be calculated as

$$k_{s,eff} = \frac{k_g \beta(1-\varepsilon_s)}{\gamma \frac{k_g}{k_s} + \varphi} \tag{15}$$

where k_g is the thermal conductivity of the gas phase assumed to be in local thermal equilibrium with the solid, k_s is the thermal conductivity of the solid material, ε_s is the bulk voidage of the solid, and β, γ, and φ are constants taken from the work of Yagi and Kunii [16]. The expression has been modified to neglect the effects of radiation heat transfer, which could become significant at elevated temperature and large particle diameters. The expression also neglects the effect of the hydrostatic force, which can improve bulk thermal conductivity.

The temperature of the sCO_2 in counter-flow configuration provides the boundary condition for the two-dimensional particle heat transfer. The second dimension is not necessary for the sCO_2 due to the heat transfer resistance being captured through a well-established fluid flow convection coefficient. The coupling between the sCO_2 and particle regions of the model can be mathematically expressed by matching the local heat flux of the two regions. The local heat flux can be expressed as

$$q''(x) = k_{s,eff} \left.\frac{dT_s}{dy}\right|_{0,x} = \frac{1}{R''}\left(T_s(0,x) - T_{CO_2}(x)\right) \tag{16}$$

where R'' is the specific thermal resistance due to the particle wall contact, heat exchanger material thermal conductivity, and sCO_2-wall convection. The resistance can be calculated as

$$R''(x) = R_c'' + \frac{t_{HX}}{k_{HX}} + \frac{1}{h_{CO_2}} \tag{17}$$

where R_c'' is the particle-wall contact resistance, which is the result of low effective thermal conductivity in the near-wall region due to increased voidage [19]. The contact resistance of the neat wall region can be calculated as

$$R_c'' = \frac{d_p}{2k_{s,eff}^{nw}} \tag{18}$$

where the thermal conductivity in the near-wall region $(k_{s,eff}^{nw})$, only considering the thin film conduction mechanism, can be calculated as

$$k_{s,\mathrm{eff}}^{\mathrm{nw}} = k_g\left(\varepsilon_w + \frac{1-\varepsilon_w}{2\Phi_w + \frac{2}{3}\frac{k_g}{k_s}}\right) \quad (19)$$

The near-wall voidage can be calculated as

$$\varepsilon_w = 1 - \frac{(1-\varepsilon_s)(0.7293 + 0.5139Y)}{1+Y} \quad (20)$$

where $Y = d_p/2a$ and a is the surface curvature.

The model has been developed in MATLAB [27] to make use of the internal ordinary differential equation solver (ODE15s), which numerically integrates the differential equations through space (x-direction). The particle region has been discretized spatially in the y-direction using a finite difference approximation, which yields a set of ordinary differential equations that can be handled by the MATLAB solver.

The nominal set of physical properties selected for the model are given in Table 1, which have been taken from experimental studies [18, 28, 29] on particulate materials for CSP application as well as heat transfer references [24]. The thermodynamic and transport properties of sCO_2 have been taken from Span et al. [30] and Vesovic et al. [31], respectively. The sCO_2 in the heat exchanger is assumed to behave in an isobaric manner at a pressure of 25 MPa.

Table 1: Physical properties of particulate and heat exchanger material

Physical Property	Value	Units
Particle diameter (d_p)	250	µm
Bulk particle density (ρ_s)	2000	kg m^{-3}
Particle specific heat $(c_{p,s})$	1200	J kg^{-1}K^{-1}
Particle material thermal conductivity (k_s)	2	W m^{-1} K^{-1}
Bulk voidage (ε_s)	0.40	-
Heat exchanger thermal conductivity (k_{HX})	23	W m^{-1} K^{-1}

The nominal simulation geometry considers a moving packed-bed with a height of 1 m and a width of 50 cm, which yields a total heat transfer area of 1.0 m^2 per channel. The gap between plates (hc_s) is set to 6 mm, which is 24 particle diameters and should be sufficient to prevent bridging. The counter-flow sCO_2 channel is taken to be 0.5 mm in width (hc_{CO_2}), which has been chosen to maintain the flow in a turbulent regime $(\mathrm{Re}_{\mathrm{Dh},CO_2} \approx 4000)$. The particle velocity is an output of the simulation, which is set to achieve an outlet temperature of 570°C for a 775°C inlet temperature. The counter-flow sCO_2 inlet velocity is set to achieve an outlet temperature of 700°C for a 550°C inlet temperature. The temperatures are set to be consistent with heat addition to a recuperated sCO_2 power cycle [3].

The moving packed-bed heat exchanger temperature profiles for the nominal simulation condition are displayed in Figure 5. The majority of the heat transfer resistance can be observed to be the result of the particle-wall convection since the temperature difference between the sCO_2 and wall is much lower than the particle and wall. The distribution of the local particle-wall convection coefficient is plotted in Figure 6. An enhanced heat transfer coefficient is observed in the first 10 cm due to the thermal entry region. After the flow is thermally developed, the local heat transfer coefficient will asymptote to a constant value around 180 W m^{-2}K^{-1}. The slight decrease in the heat transfer coefficient, after the thermal entry region, is due to the temperature dependence of the bulk particle thermal conductivity and particle-wall contact resistance. Figure 6 also displays the difference between the conventions for calculating the local particle-to-wall heat transfer coefficient (Eqns. (4) and (5)). Quantifying the particle-to-wall heat transfer coefficient based on inlet temperature (red line) results in a much lower heat transfer coefficient ($\bar{h}_{sw}$ = 50.6 W m^{-2}K^{-1}), which is not consistent with the back calculated overall heat transfer coefficient (U = 144 W m^{-2}K^{-1}) based on LMTD. The particle-to-wall heat transfer coefficient based on average solid temperature (blue line) is 182 W m^{-2}K^{-1}, which is consistent with the overall heat transfer coefficient.

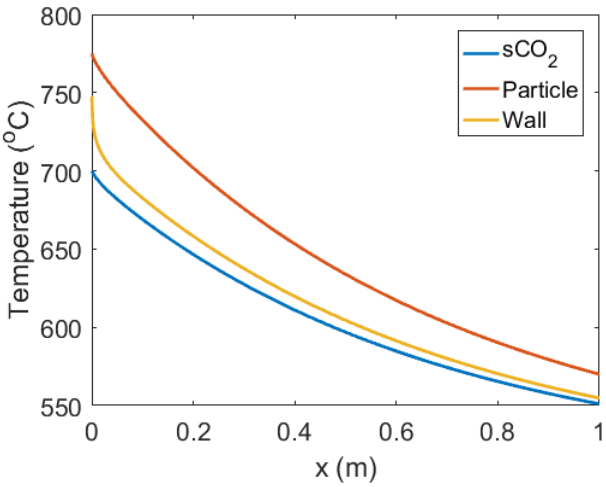

Figure 5: Profiles of the average particle, heat exchange material, and sCO_2 temperatures for the nominal moving packed-bed heat exchanger geometry

The model output provides information that can be post processed to obtain values for the total heat transfer (Q), overall heat transfer coefficient (U), average particle-wall heat transfer coefficient $(\bar{h}_{sw})$, effectiveness (ε), and number or transfer units (NTU). The heat exchanger performance metrics are reported in Table 2 for the nominal condition as well as variations in particle diameter. The nominal heat exchanger geometry is shown to be capable of transferring 5.86 kW of heat per meter squared of heat transfer area. This value could be enhanced if the effective thermal conductivity of the solid can be improved or if the particle-wall contact resistance can be reduced. Since the heat exchanger geometry is fixed, as well as the inlet and outlet

temperatures, the LMTD is fixed at 41.61°C. However, the total heat transfer and mass flow rates of particles and sCO_2 will vary as the heat transfer coefficient is affected by particle diameter. The overall heat transfer coefficient is observed to increase with decreasing particle diameter, which is due to reduction in the particle-wall contact resistance with smaller particles. The increase in particle diameter does not improve the bulk effective thermal conductivity of the particles based on the model of Yagi and Kunii [16] without considering radiation, however, the flow is much more sensitive to contact resistance in the near-wall region. Therefore, increasing particle diameter to 750 µm reduces the particle-wall convection coefficient to 139 W $m^{-2}K^{-1}$ and decreasing particle diameter to 50 µm increases the convection coefficient to 208 W $m^{-2}K^{-1}$.

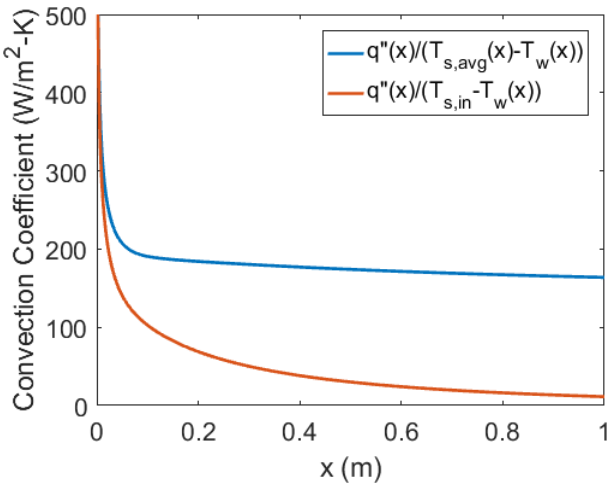

Figure 6: Local particle-to-wall heat transfer coefficients for the nominal moving packed-bed heat exchanger geometry calculated by Eqns. (4) and (5)

Table 2: Particle/sCO_2 heat exchanger performance as a function of particle diameter for a fixed 1.0 m^2 heat transfer area

Particle Diameter	250µm	50 µm	750 µm	Units
Overall HTC (U)	144	163	110	W $m^{-2}K^{-1}$
Particle-Wall HTC $(\bar{h}_{sw})$	182	208	139	W $m^{-2}K^{-1}$
Total Heat Transfer (Q)	5.86	6.63	4.50	kW
Solid Mass Flow Rate	23.8	27.0	18.3	g s^{-1}
sCO_2 Mass Flow Rate	31.3	35.4	24.0	g s^{-1}
HX Effectiveness (ε)	0.915	0.915	0.915	-
Number of Transfer Units	5.03	5.03	5.03	-

The non-dimensional heat exchanger performance metrics are also reported in Table 2. The effectiveness is observed to be 91.5% and the NTU is observed to be 5.03, which are independent of particle diameter. Since the LMTD and capacitance ratio $(\dot{m}_{CO_2} c_{p,CO_2} / \dot{m}_s c_s)$ of the heat exchanger is fixed for all of the simulations, the effectiveness and NTU will not vary. Therefore, >90% effectiveness can be expected for counter-flow sCO_2/particle heat exchangers with the operating temperatures specified. However, the heat transfer surface area required to achieve >90% effectiveness will depend on the overall heat transfer coefficient achieved by the heat exchanger geometry and particle properties.

FUTURE EXPERIMENTAL WORK

The heat exchanger models developed in the previous sections have indicated that current granular flow heat transfer correlations are not applicable to the low velocity (high residence time) flow regime of moving packed-bed heat exchangers. In order to validate the models developed here and build confidence in the design tools, an experiment is designed in in the following section to measure granular flow heat transfer coefficients in bounded domains (narrow vertical channels).

The analytical solutions presented in Figure 2 and Figure 3 as well as the particle/sCO_2 heat exchanger simulation presented in Figure 5 provide insight into the flow conditions that are desired to be studied. The experiment should be capable of making average heat transfer coefficient measurements in the range of inverse Graetz numbers from 0.025-0.075, which would correspond to solid velocities between 8.0 and 2.5 mm/s for a 10 cm tall vertical channel that is 4 mm wide with the material parameters given in Table 1.

Since the typical method of calculating heat transfer coefficients has been shown to be misleading for heat transfer in a bounded domain, it becomes imperative to assess how the heat transfer coefficient will be calculated during the experiment design process. In order to accurately quantify the average heat transfer coefficient, it is important to have knowledge of the average local particle temperature, particle mass flow rate, and local wall temperature. Making measurements of local particle temperature is difficult due to the large fluctuations that are experienced from flow inconsistencies. Therefore, an experiment with uniform constant mass flow and a methodology to determine average local particle temperature is critical for evaluation of the heat transfer coefficient.

Table 3: Parameters for moving packed-bed heat exchanger experiment design

Parameter	Value	Units
Plate spacing (hc_s)	4.0	mm
Channel length	10	cm
Channel width	5	cm
Particle mass flow	1.0-3.0	g s^{-1}
Particle velocity (v_s)	2.5-8.0	mm s^{-1}
Peclet Number (Pe_{Dh})	166.67-500	-
Inverse Graetz Number (Gz^{-1})	0.025-0.075	-

An illustration of the experiment is provided in Figure 7, which has been designed to make heat transfer coefficient measurements in moving packed-bed heat exchangers. The experiment consists of a vertical rectangular channel with heated walls on both sides. The local wall heat flux can be measured from the heater power and the local wall temperature is measured with thermocouples on the channel surface. Since the moving bed is highly insulated and the particle thermal properties are known, the average local particle temperature can be determined from an energy balance rather than a measurement. However, the

measurement should be verified against a thermocouple placed in the particle flow stream at the channel outlet. Particle mass flow rate is controlled by a volume changing lower hopper rather than sizing a discharge orifice. This approach should be capable of producing constant and uniform flow rates with various solids and operating temperatures.

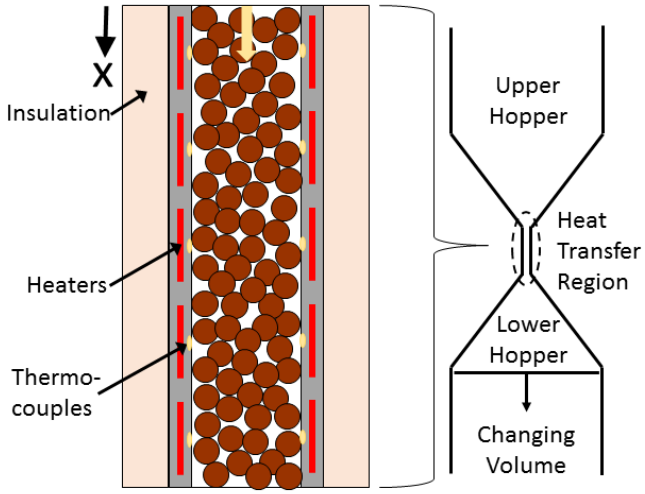

Figure 7: Illustration of moving packed-bed heat exchanger experiment for measuring heat transfer coefficients of flows with high residence times

CONCLUSION

A predictive model for the design and evaluation of a moving packed-bed heat exchanger was presented. The model is based on the single-component continuum approach previously documented in the literature. Analytical solutions of constant temperature and heat flux boundary conditions displayed Nusselt numbers, which asymptote to constant values at high residence times when solved in a bounded domain. This result is in contrast to the typical thought that the heat transfer coefficient is significantly diminished at high residence times, which is obtained from the analytical solution on a semi-infinite domain. The single-component continuum model was extended to a counter-flow particle/sCO_2 heat exchanger. The simulation results indicate that high overall heat transfer coefficients (~144 W $m^{-2}K^{-1}$) and effectiveness (>90%) are attainable in moving packed-bed heat exchangers. For the particle/sCO_2 temperatures simulated here, approximately 5.86 kW of heat can be transfer per square meter of heat transfer area. Finally, the modeling results were used to design a moving packed-bed heat exchanger experiment, which is a much smaller scale than the simulated heat exchanger, but still has the same non-dimensional characteristics. The experiment should allow for model validation and confidence in the simulated heat transfer coefficient values.

ACKNOWLEDGMENTS

The paper is based upon work supported in part by the DOE SunShot Program (SuNLaMP-0000000-1507). The authors would also like to acknowledge Ashley Byman and Robert McGillivray of Solex Thermal Science for helpful discussions on granular flow heat transfer. Sandia National Laboratories is a multi-mission laboratory managed and operated by Sandia Corporation, a wholly owned subsidiary of Lockheed Martin Corporation, for the U.S. Department of Energy's National Nuclear Security Administration under contract DE-AC04-94AL85000.

NOMENCLATURE

c_{p,CO_2}	sCO_2 specific heat capacity
$c_{p,s}$	Particle specific heat capacity
D_h	Hydraulic diameter
d_p	Particle diameter
h_{CO_2}	sCO_2-wall convection coefficient
h_{sw}	Local particle-wall convection coefficient
$\overline{h}_{sw}$	Average particle-wall convection coefficient
hc_{CO_2}	sCO_2 channel height
hc_s	Particle channel height
k_{HX}	Heat exchanger material thermal conductivity
k_s	Particle material thermal conductivity
$k_{s,eff}$	Particle effective thermal conductivity
Nu_{Dh}	Local Nusselt number based on hydraulic diameter
$\overline{Nu}_{Dh}$	Average Nusselt number based on hydraulic diameter
$\overline{Nu}_L$	Average Nusselt number based on axial flow length
Pe_L	Peclet number based on axial flow length
Q	Total heat transfer
q''	Heat flux
R''	Specific thermal resistance
R''_c	Specific particle-wall contact resistance
T_{CO_2}	sCO_2 temperature
T_s	Particle temperature
T_w	Heat exchanger wall temperature
t_{HX}	Heat exchanger material thickness
u	Convective flow velocity
U	Heat exchanger overall heat transfer coefficient
UA	Heat exchanger conductance
v_{CO_2}	sCO_2 velocity
v_s	Particle velocity

Greek

α	Thermal diffusivity

ΔT_{lm}	Log mean temperature difference
ε	Heat exchanger effectiveness
ε_{s}	Bulk particle voidage
ε_{w}	Particle near-wall voidage
$\rho_{\mathrm{CO_2}}$	sCO_2 density
ρ_{s}	Particle bulk density
τ	Residence time

REFFERENCES

[1] Z. Ma, G. Glatzmaier and M. Mehos, "Fluidized Bed Technology for Concentrating Solar Power With Thermal Energy Storage," *Journal of Solar Energy Engineering,* vol. 136, no. 3, p. 031014, 2014.

[2] Z. Ma, M. Mehos, G. Glatzmaier and B. B. Sakadjian, "Development of a concentrating solar power system using fluidized bed technology for thermal energy conversion and solid particles for thermal energy storage," *Energy Procedia,* vol. 69, pp. 1349-1359, 2015.

[3] C. S. Turchi, Z. Ma, T. W. Neises and M. J. Wagner, "Thermodynamic Study of Advanced Supercritical Carbon Dioxide Power Cycles for Concentrating Solar Power Systems," *Journal of Solar Energy Engineering,* vol. 135, no. 4, p. 041007, 2013.

[4] N. P. Siegel, C. K. Ho, S. S. Khalsa and G. J. Kolb, "Development and Evaluation of a Prototype Solid Particle Receiver: On-Sun Testing and Model Validation," *Journal of Solar Energy Engineering,* vol. 132, no. 2, p. 021008, 2010.

[5] G. Flamant, D. Gauthier, H. Benoit, J.-L. Sans, R. Garcia, B. Boissiere, R. Ansart and M. Hemati, "Dense suspension of solid particles as a new heat transfer fluid for concentrated solar thermal plants: On-sun proof of concept," *Chemical Engineering Science,* vol. 102, no. 1, pp. 567-576, 2013.

[6] C. Ho, "A review of high-temperature particle receivers for concentrating solar power," *Applied Thermal Engineering,* vol. 109, no. 1, pp. 958-969, 2016.

[7] C. K. Ho and B. D. Iverson, "Review of high-temperature central receiver designs for concentrating solar power," *Renewable and Sustainable Energy Reviews,* vol. 29, pp. 835-846, 2014.

[8] T. Baumann and S. Zunft, "Development and performance assessment of a moving bed heat exchanger for solar central receiver power plants," *Energy Procedia,* vol. 69, no. 1, pp. 748-757, 2015.

[9] H. S. Mickley and D. F. Fairbanks, "Mechanism of Heat Transfer to Fluidized Beds," *AIChE Journal,* vol. 1, no. 3, pp. 374-384, 1955.

[10] J. C. Chen, J. R. Grace and M. R. Golriz, "Heat transfer in fluidized beds: design methods," *Powder Technology,* vol. 150, no. 2, pp. 123-132, 2005.

[11] W. N. Sullivan and R. H. Sabersky, "Heat Transfer to Flowing Granular Media," *International Journal of Heat and Mass Transfer,* vol. 18, no. 1, pp. 97-107, 1975.

[12] A. O. O. Denloye and J. S. M. Botterill, "Heat Transfer in Flowing Packed Beds," *Chemical Engineering Science,* vol. 32, no. 1, pp. 461-465, 1977.

[13] J. K. Spelt, C. E. Brennen and R. H. Sabersky, "Heat Transfer to Flowing Granular Material," *International Journal of Heat and Mass Transfer,* vol. 25, no. 6, pp. 791-796, 1982.

[14] N. Obuskovic, "Heat Transfer Between Moving Beds of Solids and a Vertical Tube," PhD Thesis, 1988.

[15] M. G. Golob, "Convective Heat Transfer Performance of Sand for Thermal Energy Storage," Masters Thesis, 2011.

[16] S. Yagi and D. Kunii, "Studies on Effective Thermal Conductivities in Packed Beds," *AIChE Journal,* vol. 3, no. 3, pp. 373-381, 1957.

[17] W. L. Vargas and J. J. McCarthy, "Conductivity of granular media with stagnant interstitial fluids via thermal particle dynamics simulation," *Heat and Mass Transfer,* vol. 45, no. 24, pp. 4847-4856, 2002.

[18] T. Baumann and S. Zunft, "Properties of granular materials as heat transfer and storage medium in CSP application," *Solar Energy Materials & Solar Cells,* vol. 143, pp. 38-47, 2015.

[19] J. M. Botterill and A. O. Denloye, "A Theoretical Model of Heat Transfer to a Packed or Quiescent Fluidized Bed," *Chemical Engineering Science,* vol. 33, no. 4, pp. 509-515, 1978.

[20] S. I. Park, "Performance Analysis of a Moving-Bed Heat Exchanger in Vertical Pipes," *Energy,* vol. 21, no. 10, pp. 911-918, 1996.

[21] R. Henda and D. J. Falcioni, "Modeling of Heat Transfer in a Moving Packed Bed: Case of the Preheater in Nickel Carbonyl Process," *Journal of Applied Mechanics,* vol. 73, no. 1, pp. 47-53, 2006.

[22] T. Baumann and S. Zunft, "Theoretical and experimental investigation of a Moving Bed Heat Exchanger for Solar Central Receiver Power Plants," *6th European Thermal Sciences Conference,* vol. 395, no. 1, pp. 1-8, 2012.

[23] R. B. Bird, W. E. Stewart and N. L. Edwin, Transport Phenomena, New York: John Wiley and Sons, Inc., 2007.

[24] F. P. Incropera, D. P. Dewitt, T. L. Bergman and A. S. Lavine, Fundamentals of Heat and Mass Transfer, Hoboken: John Wiley and Sons, Inc., 2007.

[25] G. Nellis and S. Klein, Heat Transfer, New York: Cambridge University Press, 2009.

[26] H. S. Carslaw and J. C. Jaeger, Conduction of Heat in Solids, Glasgow: Oxford University Press, 1959.

[27] MathWorks, *MATLAB R2016b,* Natick, 2016.

[28] N. P. Siegel, M. D. Gross and R. Coury, "The Development of Direct Absorption and Storage Media for Falling Particle Solar Central Receivers," *Journal of Solar Energy Engineering,* vol. 137, 2015.

[29] N. Siegel, M. Gross, C. Ho, T. Phan and J. Yuan, "Physical properties of solid particle thermal energy storage media for concentrating solar power applications," *Energy Procedia,* vol. 49, no. 1, pp. 1015-1023, 2014.

[30] R. Span and W. Wagner, "A New Equation of State for Carbon Dioxide Covering the Fluid Region form the Triple-Point Temperature to 1100 K at Pressures up to 800 MPa," *Journal of Physical and Chemical Reference Data,* vol. 25, no. 6, pp. 1509-1596, 1996.

[31] V. Vesovic, W. A. Wakeham, G. A. Olchowy, J. V. Sengers, J. T. R. Watson and J. Millat, "The Transport Properties of Carbon Dioxide," *Journal of Physical and Chemical Reference Data,* vol. 19, no. 3, pp. 763-808, 1990.

[32] N. Obuskovic, "Heat Transfer Between Moving Beds of Solids and a Transverse Finned Tube," Masters Thesis, 1985.

[33] M. Colakyan, "Moving Bed Heat Transfer and Fluidized Elutriation," PhD Thesis, 1984.

[34] J. Niegsch, D. Koneke and P. M. Weinspach, "Heat Transfer and flow of bulk solids in a moving bed," *Chemical Engineering and Processing,* vol. 33, no. 1, pp. 73-89, 1994.

[35] O. Molerus, "Heat Transfer in Moving Beds with a Stagnant Interstitial Gas," *International Journal of Heat and Mass Transfer,* vol. 40, no. 17, pp. 4151-4159, 1997.

[36] H. Takeuchi, "Particles Flow Pattern and Local Heat Transfer Around Tube in Moving Bed," *AIChE Journal,* vol. 42, no. 6, pp. 1621-1626, 1996.

[37] P. Isaza, W. D. Warnica and M. Bussmann, "Thermal Performance and Sizing of Moving Bed Heat Exchangers," in *Proceedings of the ASME 2014 International Mechanical Engineering Congress and Exposition*, Montreal, 2014.

[38] S. Masamune and J. M. Smith, "Thermal Conductivity of Beds of Spherical Particles," *Industrial and Engineering Chemisty Fundamentals,* vol. 2, no. 2, pp. 136-143, 1963.